Article

Palladium-Catalyzed Enantioselective Arylation of Aryl Sulfenate Anions: A Combined Experimental and Computational Study

Tiezheng Jia, Mengnan Zhang, Samuel P McCollom, Ana Bellomo, Sonia Montel, Jianyou Mao, Spencer D. Dreher, Christopher J. Welch, Erik L Regalado, R. Thomas Williamson, Brian C Manor, Neil C. Tomson, and Patrick J Walsh

J. Am. Chem. Soc., **Just Accepted Manuscript** • Publication Date (Web): 24 May 2017

Palladium-Catalyzed Enantioselective Arylation of Aryl Sulfenate Anions: A Combined Experimental and Computational Study

Tiezheng Jia,[a] Mengnan Zhang,[a] Samuel P. McCollom,[a] Ana Bellomo,[a] Sonia Montel,[a] Jianyou Mao,[b] Spencer D. Dreher,[c] Christopher J. Welch,[c] Erik L. Regalado,[c] R. Thomas Williamson,[c] Brian C. Manor,[c] Neil C. Tomson,*[,a] Patrick J. Walsh *[,a,b]

[a]Roy and Diana Vagelos Laboratories, Penn/Merck Laboratory for High-Throughput Experimentation, Department of Chemistry, University of Pennsylvania, 231 South 34th Street, Philadelphia, Pennsylvania 19104-6323, United States, [b] Institute of Advanced Synthesis, Nanjing Tech University, 30 South Puzhu Road, Nanjing, 211816, P. R. China, [c]Department of Process Research & Development, Merck & Co., Inc., P.O. Box 2000, New Jersey 07065, United States.

ABSTRACT: A novel approach to produce chiral diaryl sulfoxides from aryl benzyl sulfoxides and aryl bromides via an enantioselective arylation of aryl sulfenate anions is reported. A (JosiPhos)Pd-based catalyst successfully promotes the asymmetric arylation reaction with good functional group compatibility. A wide range of enantioenriched diaryl, aryl heteroaryl, and even diheteroaryl sulfoxides were generated. Many of the sulfoxides prepared herein would be difficult to prepare via classic enantioselective oxidation of sulfides, including Ph(Ph-d_5)SO (90% ee, 95% yield). A DFT-based computational study suggested that chiral induction originates from two primary factors: *i*) both a kinetic and thermodynamic preference for oxidative addition that places the bromide *trans* to the JosiPhos-diarylphosphine moiety, and *ii*) Curtin-Hammett-type control over the interconversion between *O*- and *S*-bound isomers of palladium sulfenate species, following rapid interconversion between *re*- and *si*-bound transmetallation products, *re*/*si*-Pd–*O*SPh (*re*/*si*-PdO-*trans*).

Introduction

Chiral, nonracemic sulfoxides are important components of natural products,[1] synthetic bioactive compounds,[2] and marketed therapeutics, such as Nexium[3] and Armodafinil[4] (Figure 1). Sulfoxides are widely applied in agricultural chemistry[5] and polymer science.[6] Recently, they have attracted attention as promising ligands, and have been employed successfully in asymmetric catalysis.[7] Moreover, sulfoxides could serve as starting materials to construct a variety of scaffolds of great value.[8]

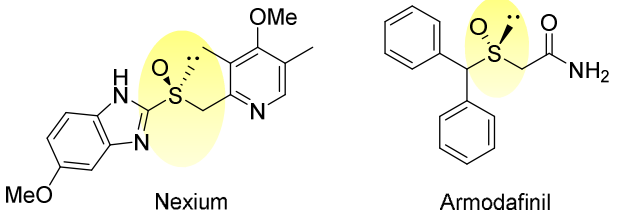

Figure 1. Selected sulfoxide-containing marketed therapeutics.

Enantioenriched sulfoxides are traditionally prepared by nucleophilic substitution with optically active sulfinate amides or esters (Scheme 1A). The classic chiral auxiliary-based Andersen procedure[9] requires diastereoselective synthesis of sulfinyl derivatives, which must be purified to remove the minor diastereomer. Overall, the procedure is tedious and can result in loss of ee in the nucleophilic substitution (Scheme 1B),[10] which is typically done with Grignard and organolithium reagents. To improve upon the Andersen method, more elaborate chiral auxiliaries and reagents have been developed, such as the Senanyake method[11] or Davis oxaziridines.[12] Nonetheless, moderate yields and enantioselectivities are obtained in some cases.[13] There are a few catalytic enantioselective approaches to synthesize sulfoxides.[9c,d] The most popular is sulfide oxidation pioneered by Kagan and Modena (Scheme 1C).[14] This approach works well for certain substrates, but gives poor results when the substituents flanking the sulfoxide are similar in size. The catalysts can exhibit low chemoselectivity, resulting in over oxidation to the sulfone and complicating purification (Scheme 1D).[15]

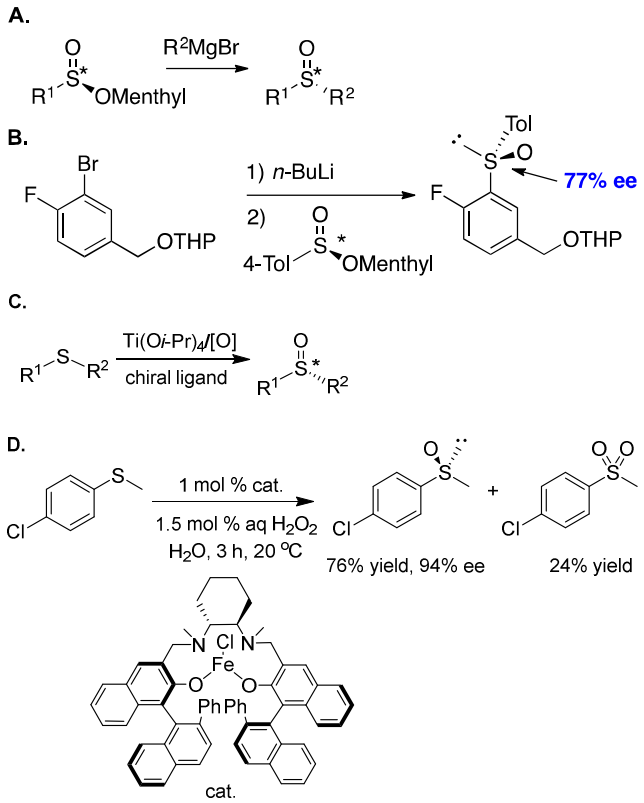

Scheme 1. Classic approaches to enantioenriched sulfoxides.

A novel approach to the synthesis of enantioenriched sulfoxides has emerged in the past decade that involves generation of sulfenate anions[16] (R–SO⁻) and their transition metal catalyzed arylations.[17] Sulfenate anions are formed *in situ* because of their highly reactive nature. Despite significant progress, the arylation strategy has focused primarily on the synthesis of racemic sulfoxides.[17] The only report of enantioselective arylation of sulfenate anions is the pioneering work of Poli and Madec in 2007 (Scheme 2a).[18] The potential utility of this approach is overshadowed by the lack of scope and low to modest enantioselectivities (0-80% ee, average 56% ee).

An innovative strategy was used by Dong, Houk and their coworkers who reported dynamic kinetic resolution (DKR) of allylic sulfoxides by combining the Mislow-Braverman-Evans rearrangement[17b] with Rh-catalyzed asymmetric hydrogenation (Scheme 2b).[19] To date this method has not been expanded beyond the synthesis of enantioenriched *n*-propyl sulfoxides. Herein, we report a palladium-catalyzed coupling of aryl sulfenate anions with aryl bromides to afford enantioenriched diaryl sulfoxides with enantioselectivities up to 98% and high yields (Scheme 2c). A computational study sheds light on the reaction pathway, and explores a unique interconversion between *O*- and *S*-bound isomers of palladium sulfenate species as the enantio-determining steps.

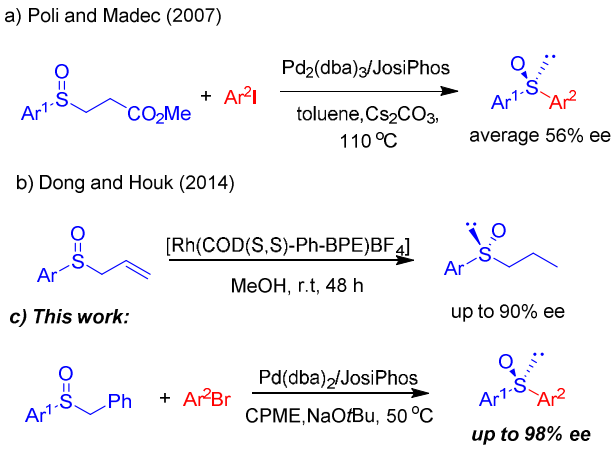

Scheme 2. Catalytic asymmetric approaches to enantioenriched diaryl sulfoxides.

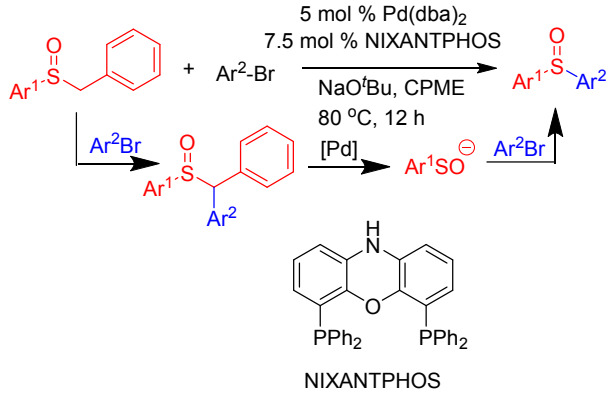

Scheme 3. Racemic diaryl sulfoxide formation from aryl benzyl sulfoxides and aryl bromides.

Results and Discussion

Catalyst Identification. We recently reported the formation of diaryl sulfoxides from aryl benzyl sulfoxides and aryl bromides via a palladium-catalyzed triple-relay cascade reaction (Scheme 3).[17d] In this process, the palladium catalyzes three different reactions–arylation of the benzylic sulfoxide, cleavage of the C–S bond and coupling of the sulfenate anion with the aryl halide. This procedure was utilized to prepare diaryl sulfoxides bearing various functional groups in excellent yields. Thus, it was viewed as a good point of departure for development of an asymmetric synthesis of diaryl sulfoxides.

The cascade reaction between benzyl phenyl sulfoxide (**1a**) and 4-*tert*-butyl bromobenzene (**2a**) was used as the test reaction. The enantioselective cross coupling reaction was initialized with ligand screen under conditions otherwise identical to the racemic diaryl sulfoxide formation (1 equiv **1a**, 2 equiv **2a**, 3 equiv NaO*t*Bu, $Pd(dba)_2$ in CPME at 80 °C for 12 h). A large library of sterically and electronically diverse enantioenriched mono- and bidentate phosphine ligands was tested. Of the 192 ligands screened, the four most

enantioselective catalysts were all JosiPhos derivatives (**L1**–**L4**, see Table 1 for structures)[20]. These four ligands were examined on larger scale, leading to excellent assay yields (94–96%, determined by ^{1}H NMR) and moderate enantioselectivities (70–75%, Table 1, entries 1 – 4, determined by chiral phase HPLC, see Supporting Information for details). Due to the lack of commercial availability of **L3**, it was not pursued. When the reaction temperature was decreased from 80 to 50 °C, the catalyst bearing the parent JosiPhos ligand, **L1**, was the most enantioselective (92% ee, 85% yield, entry 5). Ligands **L2** and **L4** exhibited enantioselectivities approximately 10% lower (entries 6 and 7) than **L1**. To further improve the yield, the equivalents of aryl bromide **2a** was increased to 3 and the reaction time was extended to 24 h, resulting in 95% assay yield with no change in ee (91%, entry 8). A survey of palladium sources, solvents, and bases resulted in inferior yields and/or enantioselectivities (see Supporting Information for details). Attempts to decrease the temperature or catalyst/ligand ratio resulted in lower yields of **3a** (entries 9 and 10). Therefore, the optimized conditions for the palladium-catalyzed enantioselective coupling reaction are: **1a** as the limiting reagent, 3 equiv **2a**, 3 equiv NaO*t*Bu base, 5 mol % $Pd(dba)_2$/7.5 mol % **L1** as the catalyst, in CPME at 50 °C for 24 h. The absolute configuration of **3a** was determined to be *R* via X-ray crystallography, and the crystal structure of **3a** is illustrated in Table 1 (see Supporting Information for details).

Table 1. Optimization of the enantioselective palladium-catalyzed coupling reaction between **1a** and **2a**. [a]

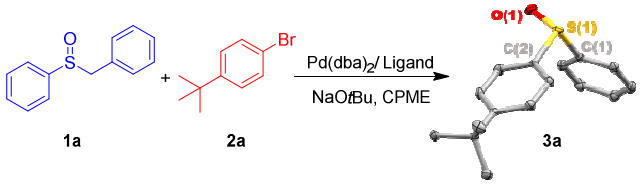

entry	ligand	catalyst/ligand loading/%	T/ °C	Assay yield/% [b]	ee /%
1	**L-1**	5/7.5	80	95	75
2	**L-2**	5/7.5	80	96	71
3	**L-3**	5/7.5	80	94	73
4	**L-4**	5/7.5	80	94	70
5	**L-1**	5/7.5	50	85	92
6	**L-2**	5/7.5	50	87	82
7	**L-4**	5/7.5	50	64	80
8[c]	**L-1**	5/7.5	50	96(95[d])	91
9[c]	**L-1**	5/7.5	40	23	91
10[c]	**L-1**	2.5/3.8	50	57	91

[a] Unless otherwise stated, reactions were carried out with **1a** (1 equiv), **2a** (2 equiv), NaO*t*Bu (3 equiv), 5 mol % $Pd(dba)_2$, 7.5 mol % ligand in CPME for 12 h. [b] Assay yields determined by ^{1}H NMR using 0.1 mmol CH_2Br_2 as internal standard. [c] 3 equiv **2a**, 24 h. [d] Isolated yield.

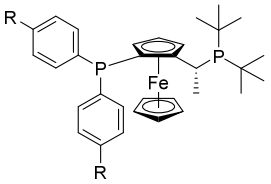

R = H, **L-1**
R = CF_3, **L-2**
R = F, **L-3**

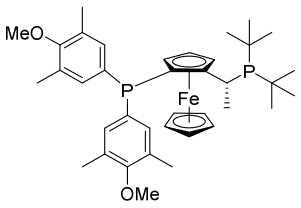

L-4

Reaction Scope. The substrate scope of aryl bromides with sulfoxide **1a** was next determined (Scheme 4). In general, a wide variety of substituted aryl or heteroaryl bromides were compatible with the optimized conditions. 2-Bromonaphthlene (**2b**) proved to be a good coupling partner, generating **3b** in 91% ee and 85% yield. Aryl bromides bearing electron-donating groups, such as 4-bromothioanisole (**2c**) or 4-bromoanisole derivatives (**2d**), were very good cross-coupling partners, giving 84–89% yield and 90–92% ee of the desired products (**3c**, **3d**). Notably, there are two different sulfur-containing functional groups (sulfoxide and sulfide) in **3c**, which would render this product difficult to prepare by traditional oxidation strategies. Electron withdrawing groups, such as 4-F, 4-Cl, 4-CF_3 and 3-OMe furnished the corresponding products (**3e**–**3h**) in 86–98% yield and 89–95% ee.

Sulfoxides with heteroaryl moieties exhibit various bioactivities, but can be difficult to prepare due to their sensitivity towards oxidizing reagents.[2] Our method is compatible with the synthesis of heteroaryl sulfoxides. Enantioenriched 3-quinolino phenyl sulfoxide (**3i**), 6-quinolino phenyl sulfoxide (**3j**) and 3-pyridyl phenyl sulfoxide (**3k**) required minor adjustments to the general conditions, such as longer reaction times (see SI). Under the modified conditions, the sulfoxide products were generated in 90–97% enantioselectivity and 84–87% yield. Of note, **3k** is the key scaffold of a series of 5-HT_{2A} antagonists in the treatment of insomnia.[2f,g] Interestingly, an aryl bromide possessing a secondary amide group (**2l**) was coupled to form the sulfoxide with good chemoselectivity, although the yield and enantioselectivity were diminished (73% yield, 76% ee). Products from Buchwald-Hartwig arylation[21] or amide α-arylation reactions[22] were not observed in this reaction. 4-Bromobenzophenone (**2m**) could also be utilized as a coupling partner under our standard conditions (85% yield, 90% ee). No products derived from 1,2-addition of the deprotonated sulfoxide to the carbonyl group were observed.

Scheme 4. Substrate scope of aryl bromides in the palladium catalyzed enantioselective arylation of sulfenate anions **1a**.

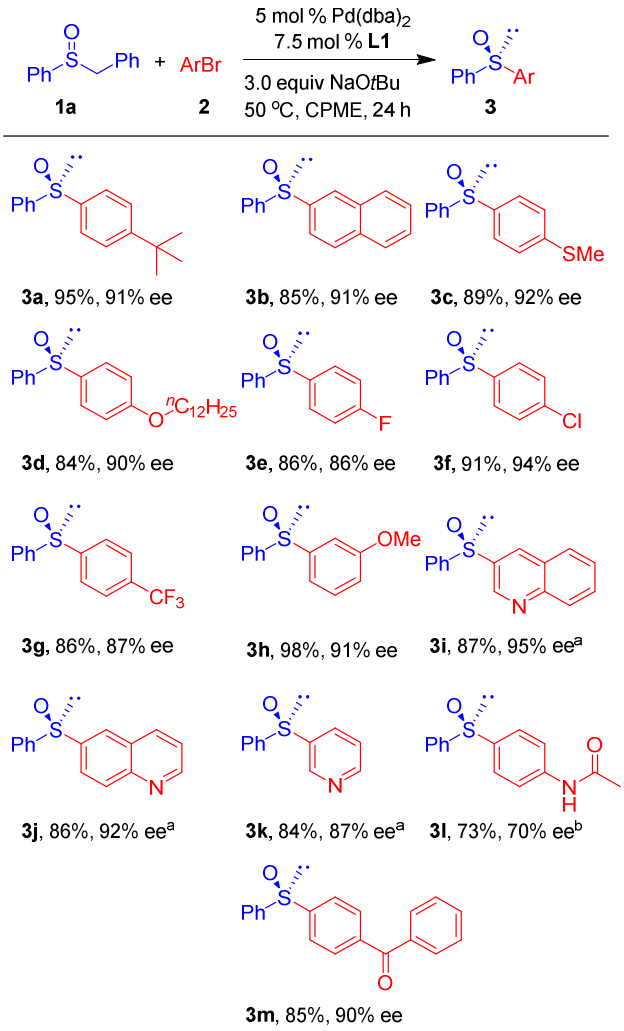

[a] 48 h reaction time. [b] 6 equiv NaO*t*Bu used.

The substrate scope of aryl benzyl sulfoxides in the arylation with bromobenzene (**2n**) was next examined (Scheme 5). Aryl benzyl sulfoxides bearing electronically neutral (2-naphthyl, **1b**) or electron-donating groups, such as 4-*tert* butyl (**1a**), 4-OMe (**1n**) and 4-NMe_2 (**1o**), were coupled providing the corresponding products in 85–95% yield with 81–94% ee. As expected, the opposite enantiomers were obtained in these coupling reactions compared to those in Scheme 4. With 4-F (**1e**), 4-Cl (**1f**), and 4-CF_3 (**1g**) substituted aryl benzyl sulfoxides, the desired products were isolated in 87–91% yield and 84–93% ee. Sterically more hindered 2-tolyl benzyl sulfoxide (**1p**) underwent coupling in 86% yield with 91% enantioselectivity. Heteroaryl sulfoxides (**3k, 3j, 3q**) bearing 3-pyridine, 3-quinolino and indole moieties were prepared via this route (83–88% yield, 81–86% ee).

Scheme 5. Substrate scope of aryl benzyl sulfoxides in the palladium-catalyzed enantioselective coupling reactions with **2n**.

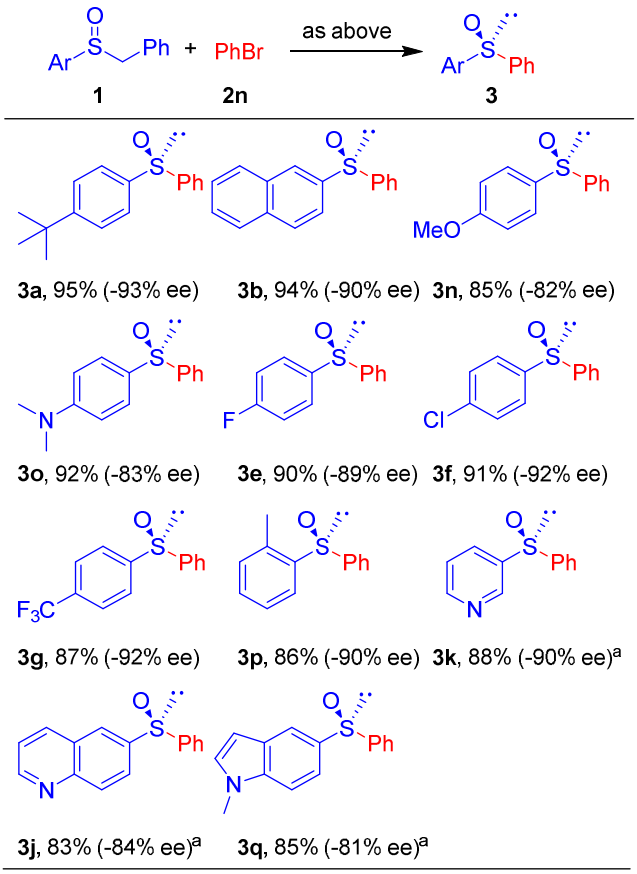

[a] 48 h reaction time.

The scalability of the *S*-arylation reaction was explored, as illustrated in Scheme 6. When 5 mmol phenyl benzyl sulfoxide **1a** (1.08 g) was coupled with 4-bromo benzophenone, the sulfoxide product **3m** was isolated in 88% yield (1.35 g) with 91% ee.

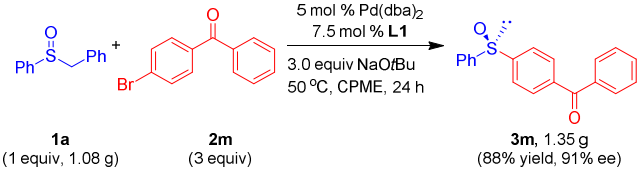

Scheme 6. Gram scale palladium-catalyzed coupling between **1a** and **2m**.

Additionally, the arylation reaction was applied to **1a** and pentadeuterobromobenzene (**2o**) to prepare enantioenriched **3r** phenyl perdeutero phenyl sulfoxide (Scheme 7). With assistance of (*R*)-(-)-1-(9-anthryl)-2,2,2-trifluoroethanol (Pirkle's alcohol)[23] as the chiral resolving agent, the ee of **3r** was determined by ^{1}H-^{13}C-HSQC and found to be 90%. Owing to the similarity of the two aryl groups, this compound could not be prepared by conventional metal-catalyzed asymmetric oxidations or chromatographic resolution approaches.

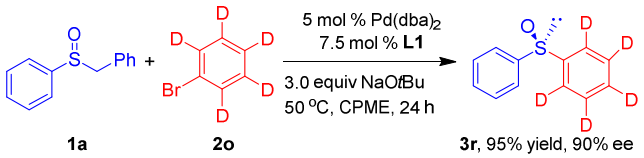

Scheme 7. Synthesis of **3r** by palladium-catalyzed arylation from **1a** and **2o**.

Diheteroaryl sulfoxides are a class of important bioactive scaffolds, yet the synthesis of these molecules remains a challenge.[2] We were pleased to find that the arylation reaction could be successfully applied to the synthesis of enantioenriched diheteroaryl sulfoxides. Simply swapping the heteroaryl groups between nucleophile and electrophile enabled the synthesis of both enantiomers of 3-quinolino 6-quinoline sulfoxide (**3s**) to be accessed from **1m** & **2j** and **1n** & **2i** under the same conditions in 82–86% yield with 85–92% ee (Scheme 8).

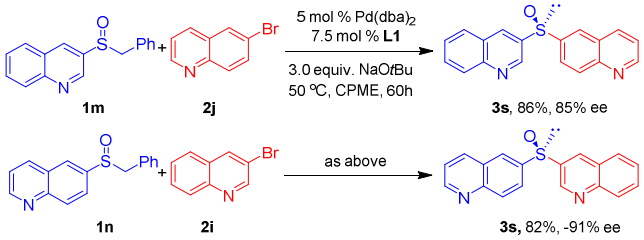

Scheme 8. Synthesis of both enantiomers of 3-quinolino 6-quinolino sulfoxide (**3s**) by palladium catalyzed arylation.

Computational Studies. Density Functional Theory (DFT) computational studies were performed to investigate the origin of the enantioselectivity provided by the (**L-1**)Pd complex. These studies employed the OLYP functional and a hybrid basis set comprised of the def2-TZVP bases for Pd (def2-SD ECP), Fe, Br, P, S, and the *ipso* carbon of the Pd-bound aryl group as well as the def2-SVP bases for all other atoms (see Supporting Information for details). In all cases, the full ligand framework was employed to capture subtle steric effects on the enantiodetermining reaction pathway. To simplify the notation in the following section, reference will be made to *i*) the *cis*/*trans* position of the $PhSO^-/Br^-$ ligand with respect to the diphenylphosphino portion of **L1** (Fig. 2, top left), *ii*) the *re*/*si*/*R*/*S* (pro)chirality of the Pd-bound $PhSO^-$ ligand (Fig. 2, bottom), and *iii*) the Fe/Me face of the complex (Fig. 2, top right), in reference to the stereochemically active backbone CpFe and Me groups of the ligand **L-1**, which lie on opposite faces of the pseudo-square-planar metal center. When investigating the oxidative addition of Ar–Br, 4-^{t}Bu-bromobenzene was used as the substrate. In all other cases, the Pd-bound aryl ligand was simplified to 4-Tol. A conductor-like screening model (COSMO) using the dielectric constant of CPME was employed when evaluating the anionic species involved in transmetallation. In contrast to related studies,[24] the application of a solvation model to the oxidative addition step was found to produce qualitatively identical results to those performed in the gas phase (see Supporting Information). Further computational work was performed on gas phase species.

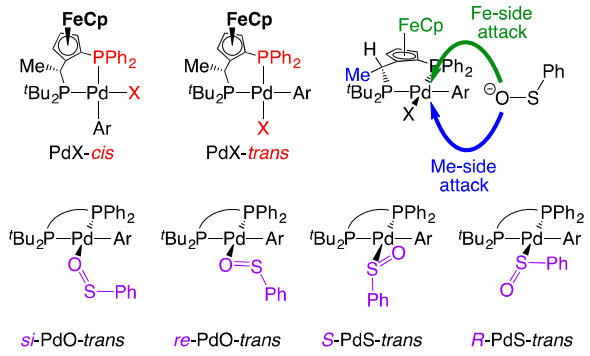

Figure 2. Graphical depiction of the nomenclature used to describe the computed isomers.

The lowest energy interaction of Ar–Br with Pd(0) involves a ArBr→Pd dative bond with Pd–Br bond distances of *ca*. 2.53 Å. This finding contrasts with related studies on less sterically demanding $L_2Pd(0)$ systems, for which binding of the arene π-system to the low-valent metal center is most favorable.[25] In the present case, η^2-binding modes, involving the *ipso*-carbon and one of its adjacent *ortho*-carbons (Pd–C bond distances range from 2.22–2.31 Å), lie *ca*. 4.5 kcal/mol higher in energy than Br-bound isomers. Multiple Pd(ArBr)-Br and Pd(ArBr)-C configurations were investigated, resulting in two primary minima for each interaction type (Figure 3), with one set constituting the precursors to *cis* oxidative addition and the other to *trans*.

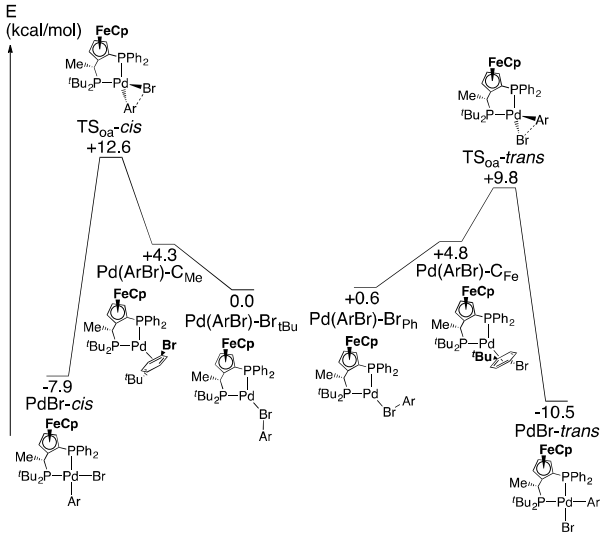

Figure 3. Energy level diagrams for ArBr oxidative addition to give PdBr-*cis* (left) and PdBr-*trans* (right).

The oxidative addition step itself was found to be facile, leading to the PdBr-*cis* and -*trans* products with energy barriers of 5.0 (*trans*) and 8.3 (*cis*) kcal/mol

relative to the arene-bound, 16 e⁻ Pd(0) complexes Pd(ArBr)-C and 9.8 (*trans*) and 12.6 (*cis*) versus Pd(ArBr)-Br. The *trans* product, as reported by the Hartwig group via X-ray crystallography,[26] lies 2.5 kcal/mol lower in energy than PdBr-*cis*, and both structures exhibit a distortion from planarity that results from the steric pressure exerted by either the Fe-side ^{t}Bu group in PdBr-*trans* or the Me-side Ph group in PdBr-*cis* (Figure 2). This distortion manifests as a 30° twist between the planes defined by P-Pd-P and C_{Ar}-Pd-Br. Reductive elimination of ArBr was also calculated to be accessible ($\Delta G^{\ddagger}$ = ~21 kcal/mol), owing to distortion of the PdBr-*cis*/*trans* complexes away from square planar geometries. Related computational studies have determined ΔG for oxidative addition from the arene-bound Pd(0) species to lie in the range of *ca*. −35 kcal/mol,[24] making the oxidative addition functionally irreversible. In the present case, the inability of the PdBr species to access square planar coordination geometries diminishes the activation energy to reductive elimination from PdBr-*cis*/*trans*. Regardless, the clear kinetic and thermodynamic preference for formation of PdBr-*trans* focused our attention on the *trans* isomer. The reaction profile resulting from PdBr-*cis* formation is described in the Supporting Information.

A COSMO solvation model was used when investigating the structures of the anionic complexes that result during transmetallation of $PhSO^-$ for Br^-. We were unable to locate pentacoordinate minima, possibly due to the presence of high energy intermediates with small energy barriers against decomposition into the square planar products. Transmetallation may also be a concerted process, which prompted us to search for transition states that may lead to stereochemical differentiation of the products. We investigated reaction coordinates resulting from consideration of i) the two open faces of the pseudo-square-planar metal center, Fe and Me, ii) the ability of the $PhSO^-$ ligand to bind through either sulfur or oxygen, and iii) the coordination of $PhSO^-$ to Pd *via* either the *si* or *re* faces of the prochiral sulfenate anion. Relaxed coordinate scans involving variations in the Pd–O/S distances allowed us to discount the four transmetallation mechanisms involving the addition of $PhSO^-$ to the Me face of PdBr-*trans*. The Fe-side ^{t}Bu group blocks Br^- from undergoing the out-of-plane distortion needed for transmetallation to occur *via* this pathway. Similar steric constraints were operative in preventing Ph*S*O transmetallation from the Fe face. Of the two remaining possible transition state orientations, the lowest energy pathway involved *re*-*O*-binding of the sulfenate anion to the Fe face of Pd ($\Delta G^{\ddagger}$ = +31.5 kcal/mol; Figure 4, bottom). This transition state structure contained a Pd–Br distance of 2.896 Å, a Pd–O distance of 2.564 Å, and a pseudo-trigonal bipyramidal coordination environment. The P_{Ph}–Pd–Br and P_{Ph}–Pd–O angles were found to be nearly identical, at 137.1° and 136.3°, respectively.

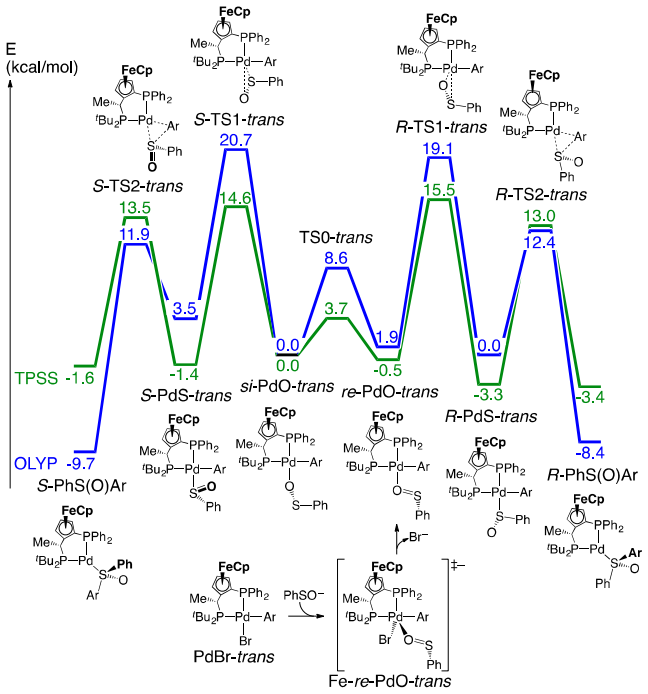

Figure 4. Energy level diagrams for *R*/*S*-ArS(O)Ph formation, calculated at the OLYP and TPSS levels of theory, following transmetallation from PdBr-*trans* (bottom, center).

The inclusion of a sodium counterion in the transmetallation step may be important for calculating an accurate activation energy, but evaluation of this more elaborate potential energy surface is beyond the scope of our current study. Doing so would require investigation into multiple modes of attack, various bridging structures, and detailed solvation models, leading to a minimum of 128 variations. We have similarly limited the scope of Pd-based leaving groups to bromide, even though other Pd–X species (e.g. Pd–O^{t}Bu) may form under the reaction conditions. We believe these to be reasonable limitations due to the steric profile of the ligand backbone, which suggests that Pd–O bond formation would be preferred over Pd–S during transmetallation. As shown below, we do not believe the stereochemistry of transmetallation to be enantiodetermining.

The preference for *re*-PdO-*trans* over *si*-PdO-*trans* formation on transmetallation was found ultimately to be unimportant as the species were determined to interconvert readily. The *re*- and *si*-PdO isomers are related by changes to the C_{Ar}–Pd–O–S and Pd–O–S–C_{Ph} dihedral angles. The C_{Ar}–Pd–O–S dihedral angle changed from 357° (*re*) to 295° (*si*) and Pd–O–S–C_{Ph} dihedral angles varied from 266° (*re*) to 122° (*si*). Multiple attempts to locate a transition state near the averages of these extremes failed, prompting us to scan the potential energy surface created by these two dihedral angles. Doing so revealed a low energy pathway involving the nearly sequential movement of the $PhSO^-$ ligand through first one dihedral angle and then the other (Fig. 5). The complex traverses *ca*. 80% of the change in the C_{Ar}–Pd–O–S dihedral angle and *ca*. 20% of the Pd–O–S–C_{Ph}

dihedral angle sweep on reaching the transition state (TSO-*trans*), which was found to lie on a broad saddle point with an imaginary frequency of –22 cm^{-1}. With an energy barrier of 8.6 kcal/mol versus *si*-PdO-*trans* and 6.7 kcal/mol vs. *re*-PdO-*trans* (ΔG favors the *si*-isomer by 1.9 kcal/mol), this low energy transition state allows the *re*- and *si*-PdO isomers to readily equilibrate (Fig. 4), thus removing transmetallation as the enantiodetermining step.

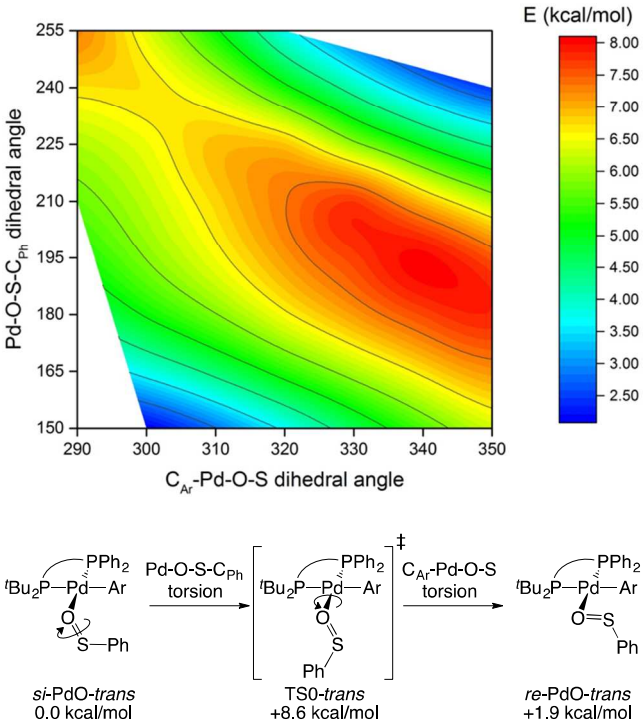

Figure 5. Top: Graphical results from a 49-point scan of the potential energy surface defined by changes to the Pd-O-S-C_{Ph} and C_{Ar}-Pd-O-S dihedral angles within PdO-*trans*. The lower left corner corresponds to *si*-PdO-*trans* and the top right to *re*-PdO-*trans*. Bottom: Depiction of the sequential torsion angle changes required for passing through TSo-*trans*.

We next considered the isomerization between the PdO and PdS isomers. Transition states were located that involved η²-binding of the S=O portion of the molecule. *S*-TS1-*trans*, which originated from *si*-PdO-*trans* (Fig. 4), has a larger activation energy ($\Delta G^{\ddagger}$ = 20.7 kcal/mol) than *R*-TS1-*trans* ($\Delta G^{\ddagger}$ = 19.1 kcal/mol). This difference is mitigated in part by the higher ground state energy of *re*-PdO-*trans* (+1.9 kcal/mol), but ultimately, the transition state isomers differ in absolute energy by 1.6 kcal/mol. Again, the Fe-side ^{t}Bu group appears to play an important role by preventing the PhSO ligand from coordinating in a mode that positions the S–O centroid (Ct_{SO}) *trans* to the diarylphosphine. Instead, the η²-bound sulfenate deviates significantly from square planarity, with the S–O centroid lying 1.47 Å from the P–Pd–P plane while subtending a Ct_{SO}–Pd–P_{Ph} angle of 139°.

Reductive elimination initially appeared as a likely point in the catalytic cycle at which stereoinduction would occur. However, reductive elimination to produce the diarylsulfoxide proceeds with $\Delta G^{\ddagger}$ = 12.4 kcal/mol for *R*-PdS-*trans* and 8.4 kcal/mol for *S*-PdS-*trans*, although the higher absolute energy of *S*-PdS-*trans* places its corresponding transition state (*S*-TS2-*trans*) only 0.5 kcal/mol below *R*-TS2-*trans* (Figure 4). Regardless, the significantly lower energy barrier to reductive elimination compared to PdO-PdS isomerization, coupled with the more facile transmetallation path to PdO formation over PdS, indicates that the stereochemical outcome of the reaction is under Curtin-Hammett control operating in the PdO-PdS interconversion step.

To test this conclusion, we sought to computationally perturb the complex in a manner that would illustrate the ability of the ligand to effect chiral induction. The persistent tetrahedral distortion of the Pd(II) complexes exhibit P–Pd–X angles as low as 145°, representing a significant deviation from the idealized value of 180° for a 16 e^{-}, d^{8} square planar species. These distortions appear to arise from steric interactions between the Ar^{-}/Br^{-}/$PhSO^{-}$ ligands and the phosphino ^{t}Bu group positioned on the Fe face of the complex. To investigate if the Fe-side ^{t}Bu group may be responsible for stereoinduction, we truncated the ^{t}Bu-based methyl group located closest to the binding site of the $PhSO^{-}$ ligand, creating a phosphine substituted with a Me-side ^{t}Bu group and an Fe-side ^{i}Pr group. Geometry optimization of the resulting *R*/*S*-PdS'-*trans* and *re*/*si*-PdO'-*trans* structures caused the S/O-donors of the $PhSO^{-}$ ligands to move toward the P_2Pd plane, generating ground state structures with greater square planar character (Table S7 in Supporting Information). Following truncation, the PPh_2–Pd–S/O angles increased by an average of 13.4°, the Pd–S/O bond lengths shortened by up to 0.29 Å, and notably, the PPh_2–Pd–Ct_{SO} angle increased by *ca.* 35° from *R*-TS1-*trans* to *R*-TS1'-*trans*, as illustrated in Figure 6. Accordingly, the $\Delta\Delta G^{\ddagger}$ between *R*- and *S*-TS1'-*trans* was found to decrease by 65%, to a value of 0.5 kcal/mol.

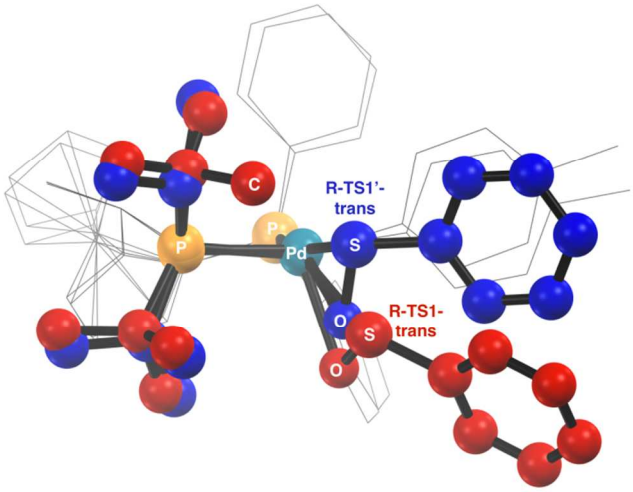

Figure 6. Structural overlay of *R*-TS1-*trans* (red) and *R*-TS1'-*trans* (blue) as optimized at the OLYP level of theory (see Supporting Information). Hydrogens have been omitted for clarity.

If the steric interaction of *R*/*S*-TS1-*trans* with the Fe-side ^{t}Bu group is in fact responsible for stereoinduction, then it would stand to reason that the less sterically encumbered *S*-TS1-*trans* isomer – with an Fe-side PhSO oxygen – would be lower in energy. This notion comports with the experimentally determined *R*-stereochemistry of the diarylsulfoxide product, suggesting that our computational model at the OLYP level of theory lacks quantitative accuracy.

Additional investigations to explore the functional dependence of the transition state energies indicated that the qualitative picture described above, in which Curtin-Hammett control in TS1 is responsible for stereoinduction, held true across a number of levels of theory. Pure, hybrid, and meta-GGA functionals (OLYP, O3LYP, TPSS, TPSSo, B3LYP) were screened. In all cases, TS1 was found to be enantiodetermining, and two of them (TPSS, TPSSh) predicted a lower relative energy for *S*-TS1-*trans*, which would lead to the *R*-diarylsulfoxide product (Figure 4; see Supporting Information). As seen for *R*-TS1-*trans* in Figure 6, the steric imposition of the Fe-side ^{t}Bu group would be expected to influence the structure of *S*-TS1-*trans* preventing the PhSO unit from binding to the metal center in a symmetric fashion with respect to the square planar coordination environment. However, while the OLYP functional predicted a lower energy for the isomer that placed the more sterically demanding atom (S) next to the chiral-inducing ^{t}Bu group, the experimentally consistent TPSS(o) results indicate that the lower energy TS1 isomer (*S*-TS1-*trans*) will place the sterically least demanding PhSO atom (O) next to the Fe-side ^{t}Bu group. Thus, computational work at the OLYP level of theory provided a qualitatively accurate picture, from which a near-quantitatively correct view of the reaction profile could be accessed by evaluating the performance of various functionals at the enantiodetermining portion of the reaction manifold.

Conclusions

In summary, a catalytic asymmetric method to synthesize enantioenriched diaryl sulfoxides from aryl benzyl sulfoxides and aryl bromides via a palladium-catalyzed arylation of aryl sulfenate anions is described. The reaction can be classified as a dynamic kinetic asymmetric transformation (DyKAT), because the palladium obliterate the stereocenter of the racemic aryl benzyl sulfoxide starting material.[27] In contrast to S–O bond formation in the traditional chiral oxidation of sulfides, the C(sp^2)-S bond is formed in this approach. Thus, it offers a complimentary pathway to produce a vast array of diaryl sulfoxides, some of which would be a formidable challenge to prepare via previous catalytic enantioselective reactions.

A computational study provides the first mechanistic insights into the dynamic processes between sulfenate anions and transition metals in enantioselective arylations of these reactive species. DFT calculations indicate that two primary factors lead to the high degree of experimental control over the stereochemical outcome of the reaction. First, the oxidative addition step favors the formation of PdBr-*trans*, in which the bromide is placed *trans* to the PPh_2 portion of the chiral diphosphine ligand. In so doing, the bromide and the subsequent sulfenate ligand are forced to lie *cis* to the sterically encumbering ^{t}Bu groups of the P^{t}Bu$_2$ portion of the diphosphine. Once formed, the *O*-bound sulfenate complex was found to isomerize to the *S*-bound sulfenate species through an eta^2-*S*,*O*-bound transition state under Curtin-Hammett-type control.

We envision that our enantioselective palladium-catalyzed arylation will be of great interest in the medicinal chemistry and the synthesis of enantioenriched sulfoxides ligands. We expect that insight gained from our computational studies will be of use to those considering the multiple mechanisms by which chiral ligands can induce stereochemical control in complex catalytic cycles.

ASSOCIATED CONTENT

Supporting Information. Procedures and full characterization of new compounds, crystallographic data (CIF). This material is available free of charge via the Internet at http://pubs.acs.org.

AUTHOR INFORMATION

Corresponding Author

*pwalsh@sas.upenn.edu, *tomson@upenn.edu

Notes

The authors declare no competing financial interest.

ACKNOWLEDGMENT

We thank the National Science Foundation (CHE-1464744) for financial support.

REFERENCES

1. a) Dini, I.; Tenore, G. C.; Dini, A. *J. Nat. Prod.* **2008**, *71*, 2036; b) El-Aasr, M.; Fujiwara, Y.; Takeya, T.; Tsukamoto, S.; Ono, M.; Nakamo, D.; Okawa, M.; Kinjo, J.; Yoshimitsu, H.; Nohara, T. *J. Nat. Prod.* **2010**, *73, 1306;* c) Wyche, T. P.; Piotrowski, J. S.; Hou, Y.; Braun, D.; Deshpande, R.; McIlwain, S.; Ong, I. M.; Myers, C. L.; Guzei, I. A.; Westler, W. M.; Andes, D. R.; Bugni, T. S. *Angew. Chem., Int. Ed.* **2014**, *53*, 11583; d) Nohara, T.; Fujiwara, Y.; Komota, Y.; Kondo, Y.; Saku, T.; Yamaguchi, K.; Komohara, Y.; Takeya, M. *Chem. Pharm. Bull.* **2015**, *63*, 117.
2. a) Rinehart, K. L.; Sakai, R. US2004/59112 A1, **2004**; b) Amira Pharmaceuticals Inc., US/2010/4331 A1, **2010**; c) Amira Pharmaceuticals Inc., Hutchinson, J. H.; Seiders, T. J.; Arruda, J. M.; Roppe, J. R. WO2010/42652 A2, **2010**; d)

Combinatorx (Singapore) Pte. Ltd., US2010/9970 A1, **2010**; e) GLAXOSMITHKLINE LLC; Banka, A. J.; Botyanszki, J.; Duan, M.; Leivers, M. R.; Shotwell, J. B.; Tallant, M. D.; Dickerson, S. H.; Tai, V. W.-F.; McFadyen, R. B.; Redman, A. M.; Yu, J.; Li, X.; Garrido, D. M.; Catalano, J. G.; Adjabeng, G. Patent: WO2012/87938 A1, **2012**; f) Merck Sharp and Dohme Limited, Patent: WO2006/21805A1, 2006; g) Wilson, K. J.; van Niel, M. B.; Cooper, L.; Bloomfield, D.; O'Conner, D.; Fish, L. R.; MacLeod, A. M. *Bioorg. Med. Chem. Lett.* **2007**, *17*, 2643.

3. Astra Aktiebolag, US5877192 A, 1998.
4. Engber, T. M.; Koury, E. J.; Dennis, S. A.; Miller, M. S.; Contreras, P. C.; Bhat, R. V. *Neurosci. Lett.* **1998**, *241*, 95.
5. a) Buronfosse, T.; Moroni, P.; Benoît, E.; Rivière, J. L.; *J. Biochem. Toxicol.* **1995**, *10*, 179; b) Le, D. T.; Tarrago, L.; Watanabe, Y.; Kaya, A.; Lee, B. C.; Tran, U.; Nishiyama, R.; Fomenko, D. E.; Gladyshev, V. N.; Tran, L.-S. P. *PLoS ONE*, **2013**, *8*, e65637.
6. a) Oyama, T.; Naka, K.; Chujo, Y. *Macromolecules* **1999**, *32*, 5240; b) Numata, M.; Aoyagi, Y.; Tsuda, Y.; Yarita, T.; Takatsu, A. *Anal. Chem.* **2008**, *80*, 509.
7. For reviews, see: a) Trost, B. M.; Rao, M. *Angew. Chem., Int. Ed.* **2015**, *54*, 5026; b) Sipos, G.; Drinkel, E. E.; Dorta, R. *Chem. Soc. Rev.* **2015**, *44*, 3834; c) Mellah, M.; Voituriez, A.; Schulz, E. *Chem. Rev.* **2007**, *107*, 513; d) Otocka, S.; Kwiatkowska, M.; Madalińska, L.; Kiełbasiński, P. *Chem. Rev.* **2017**, *117*, 4147. For recent examples, see: e) Chen. J.; Chen, J.; Lang, F.; Zhang, X.; Cun, L.; Zhu, J.; Deng, J.; Liao, J. *J. Am. Chem. Soc.* **2010**, *132*, 4552. f) Dorman, P. K.; Leung, P. L.; Dong, V. M. *Tetrahedron* **2011**, *67*, 4378; g) Trost, B. M.; Ryan, M. C.; Rao, M.; Markovic, T. Z. *J. Am. Chem. Soc.* **2014**, *136*, 17422. h) Yang, T.; Zhang, Y.; Cao, P.; Wang, M.; Li, L.; Li, D.; Liao, J. *Tetrahedron* **2016**, *72*, 2707; i) Chen, B.; Cao, P.; Yin, X.; Liao, Y.; Jiang, L.; Ye, J.; Wang, M.; Liao, J. *ACS Catal.* **2017**, *7*, 2425.
8. For review, see: a) Shafir, A. *Tetrahedron Lett.* **2016**, *57*, 2673. For recent examples, see: b) Eberhart, A. J.; Procter, D. J. *Angew. Chem., Int. Ed.* **2013**, *52*, 4008; c) Peng, B.; Huang, X.; Xie, L.-G.; Maulide, N. *Angew. Chem., Int. Ed.* **2014**, *53*, 8718; d) Eberhart, A. J.; Shrives, H. J.; Alvarez, E.; Carrer, A.; Zhang, Y.; Procter, D. J. *Chem. Eur. J.* **2015**, *21*, 7428; e) Kaldre, D.; Maryasin, B.; Kaiser, D.; Gajsek, O.; Gonzalez, L.; Maulide, N. *Angew. Chem., Int. Ed.* **2017**, *56*, 2212; f) Huang, X.; Patil, M.; Fares, C.; Thiel, W.; Maulide, N. *J. Am. Chem. Soc.* **2013**, *135*, 7312; g) Fernández-Salas, J. A.; Eberhart, A. J.; Procter, D. J. *J. Am. Chem. Soc.*, **2016**, *138*, 790; h) Shang, L.; Chang, Y.; Luo, F.; He, J.-N.; Huang, X.; Zhang, L.; Kong, L.; Li, K.; Peng, B. *J. Am. Chem. Soc.*, **2017**, *139*, 4211.
9. For pioneering work, see: a) Andersen, K. K. *Tetrahedron Lett.* **1962**, 93; b) Andersen, K. K.; Gaffield, W.; Papanikolaou, N. E.; Foley, J. W.; Perkins, R. I. *J. Am. Chem. Soc.* **1964**, *86*, 5637. For reviews, see: c) Wojaczyńska, E.; Wojaczyński, J. *Chem. Rev.* **2010**, *110*, 4303; d) O'Mahony, G. E.; Kelly, P.; Lawrence, S. E.; Maguire, A. R. *Arkivoc* **2011**, *1*, 1; c) Bolm, C. *Coord. Chem. Rev.* **2003**, *237*, 245.
10. Takiguchi, H.; Ohmori, K.; Suzuki, K. *Angew. Chem., Int. Ed.* **2013**, *52*, 10472.
11. a) Han, Z.; Krishnamurthy, D.; Grover, P.; Wilkinson, H. S.; Fang, Q. K.; Su, X.; Lu, Z.-H.; Magiera, D.; Senanyake, C. H. *Angew. Chem., Int. Ed.* **2003**, *42*, 2032; b) Han, Z.; Song, J. J.; Yee, N. K.; Xu, Y.; Tang, W.; Reeves, J. T.; Tan, Z.; Wang, X.-J.; Lu, B.; Krishnamurthy, D.; Senanayake, C. H. *Org. Process Res. Dev.* **2007**, *11*, 605.
12. For reviews, see: a) Williamson, K. S.; Michaelis, D. J.; Tehshik P. Yoon, T. P. *Chem. Rev.* **2014**, *114*, 8016. For pioneering works, see: b) Davis, F. A.; Sheppard, A. C. *Tetrahedron* **1989**, *45*, 5703; c) Davis, F. A.; Stringer, O. D. *J. Org. Chem.* **1982**, *47*, 1774; d) Davis, F. A.; Chattopadhyay, S.; Towson, J. C.; Lal, S.; Reddy, T. *J. Org. Chem.* **1988**, *53*, 2087. For Davis oxaziridines used in the synthesis of proton pump inhibitors, see: e) Mahale, R. D.; Rajput, M. R.; Maikap, G. C.; Gurjar, M. K. *Org. Process Res. Dev.* **2010**, *14*, 1264.
13. Lumbroso, A.; Cooke, M. L.; Breit, B. *Angew. Chem., Int. Ed.* **2013**, *52*, 1890.
14. a) Pitchen, P.; Dunach, E.; Deshmukh, M. N.; Kagan, H. B. *J. Am. Chem. Soc.* **1984**, *106*, 8188. b) Di Furia, F.; Modena, G.; Seraglia, R. *Synthesis* **1984**, 325.
15. Egami, H.; Katsuki, T. *J. Am. Chem. Soc.* **2007**, *129*, 8940.
16. For reviews, see: a) O'Donnell, J. S.; Schwan, A. L. *J. Sulfur. Chem.* **2004**, *25*, 183; b) Maitro, G.; Prestat, G.; Madec, D.; Poli, G. *Tetrahedron: Asymmetry* **2010**, *21*, 1075; c) Schwan, A. L.; Söderman, S. C. *Phosphorus, Sulfur Silicon, Relat. Elem.* **2013**, *188*, 275; for sulfenate anions as catalyst, see: d) Zhang, M.; Jia, T.; Yin, H.; Carroll, P. J.; Schelter, E. J.; Walsh, P. J. *Angew. Chem., Int. Ed.* **2014**, *53*, 10755; e) Zhang, M.; Jia, T.; Sagamanova, I. K.; Pericas, M. A.; Walsh, P. J. *Org. Lett.* **2015**, *17*, 1164; f) Zhang, M.; Jia, T.; Wang, C. Y.; Walsh, P. J. *J. Am. Chem. Soc.* **2015**, *137*, 10346; for sulfenate anions in enantioselective alkylation, see: g) Zhong, L.; Ban, X.; Kee, C. W.; Tan, C.-H. *Angew. Chem,. Int. Ed.* **2014**, *53*, 11849. For visible-light accelerated metal-free Friedel-Crafts-type sulfinylation, see: h) Meyer, A. U.; Wimmer, A.; Kçnig, B. *Angew. Chem,. Int. Ed.* **2017**, *56*, 409.
17. a) Maitro, G.; Vogel, S.; Prestat, G.; Madec, D.; Poli, G. *Org. Lett.* **2006**, *8*, 5951; b) Bernoud, E.; Le Duc, G.; Bantreil, X.; Prestat, G.; Madec, D.; Poli, G. *Org. Lett.* **2010**, *12*, 320; c) Izquierdo, F.; Chartoire, A.; Nolan, S. P. *ACS Cat.* **2013**, *3*, 2190; d) Jia, T.; Bellomo, A.; Montel, S.; Zhang, M.; El Baina, K.; Zheng, B.; Walsh, P. J. *Angew. Chem., Int. Ed.* **2014,** *53*, 260; e) Jia, T.; Zhang, M.; Sagamanova, I. K.; Wang, C. Y.; Walsh, P. J. *Org. Lett.* **2015**, *17*, 1168; f) Gelat, F.; Lohier, J.-F.; Gaumont, A.-C.; Perrio, S. *Adv. Synth. Catal.* **2015**, *357*, 2011; g) Jia, T.; Zhang, M.; Jiang, H.; Wang, C. Y.; Walsh, P. J. *J. Am. Chem. Soc.* **2015**, *137*, 13887; h) Jiang, H.; Jia, T.; Zhang, M.; Walsh, P. J. *Org. Lett.* **2016**, *18*, 972.
18. Maitro, G.; Vogel, S.; Sadaoui, M.; Prestat, G.; Madec, D.; Poli, G. *Org. Lett.* **2007**, *9*, 5493.
19. Dornan, P. K.; Kou, K. G. M.; Houk, K. N.; Dong, V. M. *J. Am. Chem. Soc.* **2014**, *136*, 291.
20. For review, see: a) Blaser, H.-U.; Brieden, W.; Pugin, B.; Spindler, F.; Studer, M.; Togni, A. *Top. Catal.* **2002**, *19*, 3. For pioneering works, see: b) Togni, A.; Häusel, R. *Synlett* **1990**, 633; c) Togni, A.; Rihs, G.; Blumer, R. E. *Organometallics* **1992,** *11*, 613; d) Pugin, B.; Müller, M.; Spindler, F. EP 0496699, 1992, assigned to Ciba-Geigy; Pugin, B. EP 0728768, 1996, assigned to Ciba-Geigy; Pugin, B. WO 96/32400, 1996, assigned to Novartis; Pugin, B.; Landert, H. WO 98/01457, 1998, assigned to Novartis.
21. a) Surry, D. S.; Buchwald, S. L. *Chem. Sci.* **2010**, *1*, 13; b) Surry, D. S.; Buchwald, S. L. *Chem. Sci.* **2011**, *2*, 27; c) Hartwig, J. F. *Acc. Chem. Res.* **2008**, *41*, 1534; d) Evano, G.; Blanchard, N.; Toumi, M. *Chem. Rev.* **2008**, *108*, 3054.
22. a) Zheng, B.; Jia, T.; Walsh, P. J. *Org. Lett.* **2013**, *15*, 4190; b) Zheng, B.; Jia, T.; Walsh, P. J. *Adv. Synth. Catal.* **2014**, *356*, 165.
23. Pirkle, W. H.; Sikkenga, D. L.; Pavlin, M. S. *J. Org. Chem.* **1977**, *42*, 384.
24. Senn, H. M.; Ziegler, T. *Organometallics* **2004**, *23*, 2980.
25. a) Albert, K.; Gisdakis, P.; Rösch, N. *Organometallics* **1998**, *17*, 1608; b) Sundermann, A.; Martin, J. M. L. *Chem. Eur. J.* **2001**, *7*, 1703; c) Jakt, M.; Johanissen, L.; Rzepa, H. S.; Widdowson, D. A.; Wilhelm, R. *J. Chem. Soc., Perkin Trans. 2* **2002**, 576.

26. Roy, A. H.; Hartwig, J. F. *J. Am. Chem. Soc.* **2003**, *125*, 8704
27. Walsh, P. J.; Kozlowski, M. C. *Fundamentals of Asymmetric Catalysis*; University Science Books: Sausalito, CA, 2009.

Insert Table of Contents artwork here